Close-coupling calculations for the electron-impact excitation of Zn^+

M. S. Pindzola, N. R. Badnell, and R. J. W. Henry
Department of Physics, Auburn University, Auburn, Alabama 36849

D. C. Griffin
Department of Physics, Rollins College, Winter Park, Florida 32789

W. L. van Wyngaarden
Department of Physics, California Polytech State University, San Luis Obispo, California 93407
(Received 19 April 1991)

Electron-impact-excitation cross sections for Zn^+ are calculated in a multiple-*LS*-term close-coupling approximation. Total cross sections for the $4s \rightarrow 4p$ transition are compared with crossed-beams [Rogers *et al.*, Phys. Rev. A **25**, 681 (1982)] and merged-beams [Smith *et al.*, Phys. Rev. Lett. **67**, 30 (1991)] experiments. Taking into account cascade effects, the close-coupling calculations and the crossed-beams measurements are found to be in reasonable agreement over a wide energy range. When only the forward-angle part of the cross section is calculated, good agreement with the merged-beams measurements is found near the excitation threshold, but at the higher energies the experimental value is somewhat lower than the theory predicts.

PACS number(s): 34.80.Kw

I. INTRODUCTION

The study of electron-ion collision processes forms the basis of our understanding of a wide variety of astrophysical and laboratory plasmas. One of the most successful theoretical methods for calculating excitation cross sections is to solve a set of close-coupled equations derived from an eigenfunction expansion of the target-ion wave function [1–10]. Direct tests of the close-coupled method's prediction for excitation cross sections are now being provided by a growing number of atomic-collision experiments [11–13].

In this paper we compare close-coupling calculations for the $4s \rightarrow 4p$ excitation cross section of Zn^+ with both a recent merged-beams experiment [14] and an earlier crossed-beams experiment [15]. Since a previous 5-state close-coupling calculation [16] for Zn^+ did not cover the crucial threshold energy region below 15 eV, in which relatively weak resonance structures appear, we have made new close-coupling calculations to compare directly with the two experiments. In the case of the merged-beams experiment [14], we are forced to examine not only a $0°-180°$ total cross section, but also a $0°-90°$ partial cross section. Since the two experiments differ by almost

TABLE I. Energy levels for Zn^+ (relative to the ground state in eV).

	LS term	Configuration-interaction SUPERSTRUCTURE (present work)	Configuration-interaction CIV3 (Msezane and Henry, Ref. [16])	Experiment (Moore, Ref. [20])
1	$3d^{10}4s\ ^2S^e$	0.00	0.00	0.00
2	$3d^{10}4p\ ^2P^o$	5.71	6.48	6.08
3	$3d^9 4s^2\ ^2D^e$	8.23	10.99	7.91
4	$3d^{10}5s\ ^2S^e$	11.07	11.33	10.96
5	$3d^{10}4d\ ^2D^e$	12.12	11.69	12.02
6	$3d^{10}5p\ ^2P^o$	12.57		12.59
7	$3d^9 4s4p\ ^4P^o$	12.71		12.98
8	$3d^9 4s4p\ ^4F^o$	12.97		13.27
9	$3d^9 4s4p\ ^4D^o$	13.44		13.88
10	$3d^9 4s4p\ ^2P^o$	14.19		14.07
11	$3d^9 4s4p\ ^2D^o$	13.88		14.20
12	$3d^9 4s4p\ ^2F^o$	13.62		14.16
13	$3d^9 4s4p\ ^2P^o$	17.01		16.16
14	$3d^9 4s4p\ ^2D^o$	17.24		16.32
15	$3d^9 4s4p\ ^2F^o$	16.82		

TABLE II. $4s \rightarrow 4p$ oscillator strengths for Zn^+.

Method	Oscillator strength Length	Velocity
Configuration-interaction SUPERSTRUCTURE (present work)	0.855	0.802
Configuration-interaction CIV3 (Msezane and Henry, Ref. [16])	0.699	0.699
Multiconfiguration Hartree-Fock (Froese-Fischer, Ref. [21])	0.732	0.839

a factor of 2 at the higher energies, we also reexamine the old 5-state results [16] in the light of the new close-coupling calculations. In Sec. II we discuss in detail our calculational methods; Sec. III compares theory with experiment where possible; and Sec. IV contains a brief summary.

II. CALCULATIONAL METHODS

Bound-state wave functions, energies, and oscillator strengths for Zn^+ were calculated in LS coupling using a modified version of the code SUPERSTRUCTURE [17]. The radial orbitals for Zn^+ were generated by solving for them in a local model potential, itself generated by Slater-type-orbitals according to the prescription of Burgess, Mason, and Tully [18]. To fix properly the energy positions of resonance structures in the subsequent scattering calculation, it is important to have reasonable energy levels for all the low-lying states of the target. Within the context of a configuration-interaction calculation for 15 LS terms, the radial orbitals for Zn^+ were optimized by varying a radial scaling parameter on the model potential to minimize a weighted sum of eigenenergies. Of particular difficulty were the energy positions of the $3d^{10}4p$ and $3d^9 4s^2$ excited states relative to the $3d^{10}4s$ ground state. Our energy levels for the low-lying LS terms in Zn^+ are given in Table I and compared with both previous atomic structure calculations [16] using the code CIV3 [19] and experimental observations [20]. The energies obtained by the method discussed are an improvement over those obtained previously [16]. Another gauge of the accuracy of the target wave functions is the evaluation of the $4s \rightarrow 4p$ oscillator strength. Length and velocity forms are compared for three different theoretical calculations in Table II. The most reliable oscillator strength is probably the length form from the multiconfiguration Hartree-Fock calculation of Froese-Fischer [21].

Collision cross sections were calculated in a multiple-LS-term close-coupling approximation using the latest version of the code RMATRX [5,22]. In the R-matrix method [4] the $(N+1)$-electron wave function is expanded in the inner region in terms of a finite set of bound-continuum and bound-bound functions, the latter being included to satisfy the orthogonality conditions imposed on the former and optionally included to allow for correlation. The continuum function is additionally expanded in terms of a finite set of basis functions which facilitates the solution of the resonant-scattering problem at many energies. The expansion coefficients are determined by the diagonalization of the $(N+1)$-electron Hamiltonian

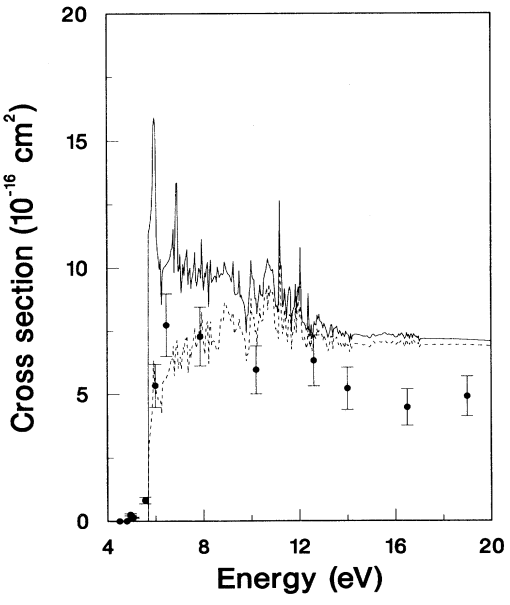

FIG. 1. Total and partial cross section for $4s \rightarrow 4p$ transition. Solid curve, 0°—180° total cross section in 15-state close-coupling calculation; dashed curve, 0°—90° partial cross section in 15-state close-coupling calculation; solid circles, merged-beams experiment (Ref. [14]).

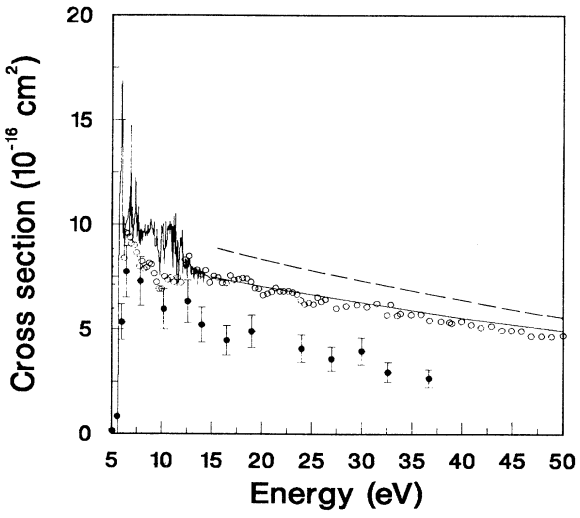

FIG. 2. Total cross section for $4s \rightarrow 4p$ transition. Solid curve, 15-state close-coupling calculation; dashed curve, 15-state close-coupling calculation with cascade enhancement; solid circles, merged-beams experiment (Ref. [14]); open circles, crossed-beams experiment (Ref. [15]).

TABLE III. $4s \rightarrow 4p$ excitation cross sections for Zn^+.

Method	Cross section (10^{-16} cm^2) 15 eV	20 eV	40 eV	50 eV
15-state close-coupling using SUPERSTRUCTURE target (present work)	7.41	7.04	5.54	4.96
5-state close-coupling using CIV3 target (present work)	5.57	5.20	4.53	4.10
5-state close-coupling using CIV3 target (Msezane and Henry, Ref. 16)	4.31	3.98	3.34	3.06

within the inner region and by the imposition of suitable boundary conditions. The latest version of the code RMATRX [22] includes routines to solve the asymptotic coupled equations perturbatively [23] and to "top-up" total dipole collision strengths from high partial waves [24,25].

III. COMPARISON OF THEORY AND EXPERIMENT

We compare a 15-state close-coupling calculation for the $4s \rightarrow 4p$ excitation cross section of Zn^+ with a recent merged-beams experiment [14] in Fig. 1. This calculation includes all 15 LS terms listed in Table I with configuration interaction between all terms of the same symmetry. The relatively weak resonance structures seen in the threshold region are typical of strong dipole transitions. Since the experiment only measures the cross section at forward-scattering angles, we present the 15-state results in Fig. 1 as a total cross section from $0°-180°$ and as a partial cross section from $0°-90°$. Since there is no convenient algebraic reduction, we obtain the partial cross section by first calculating [26] the angular differential cross sections and then numerically integrating the results from $0°-90°$. The three experimental points at 6.0, 6.5, and 7.9 eV are found to be in good agreement with the 15-state partial-cross-section results. As shown in Fig. 1, the total and partial cross sections merge together between 10 and 12 eV. The merged-beams measurements at 12.6 eV and above can thus be regarded as total cross-section data.

Over an extended energy range we compare the 15-state close-coupling calculation for the $4s \rightarrow 4p$ cross section of Zn^+ with both the merged-beams experiment [14] and an earlier crossed-beams experiment [15] in Fig. 2. Resonance structures in the total cross section are confined to energies below the 18.0-eV ionization threshold. For incident energies greater than the $3d^{10}5s$ excitation threshold at 11 eV, contributions from radiative cascade are present in the crossed-beams measurements. The dashed line in Fig. 2 shows the 15-state close-coupling results allowing for the cascade enhancement. As shown by Burgess and Tully [27], using the Coulomb-

TABLE IV. $4s \rightarrow 4p$ cascade factors for Zn^+ at 40-eV incident energy.

Method	Cross sections (10^{-16} cm^2) $\sigma(4s \rightarrow 4p)$	$\sigma(4s \rightarrow 5s)$	$\sigma(4s \rightarrow 4d)$	$\mathcal{F}^a$
15-state close-coupling using SUPERSTRUCTURE target (present work)	5.54	0.12	0.43	1.18
5-state close-coupling using CIV3 target (present work)	4.53	0.34	0.76	1.41
5-state close-coupling using CIV3 target (Msezane and Henry, Ref. [16])	3.34	0.37	0.58	1.46

[a] $\mathcal{F} = \dfrac{\sigma(4s \rightarrow 4p) + \sigma(4s \rightarrow 5s) + 2\sigma(4s \rightarrow 4d)}{\sigma(4s \rightarrow 4p)}$.

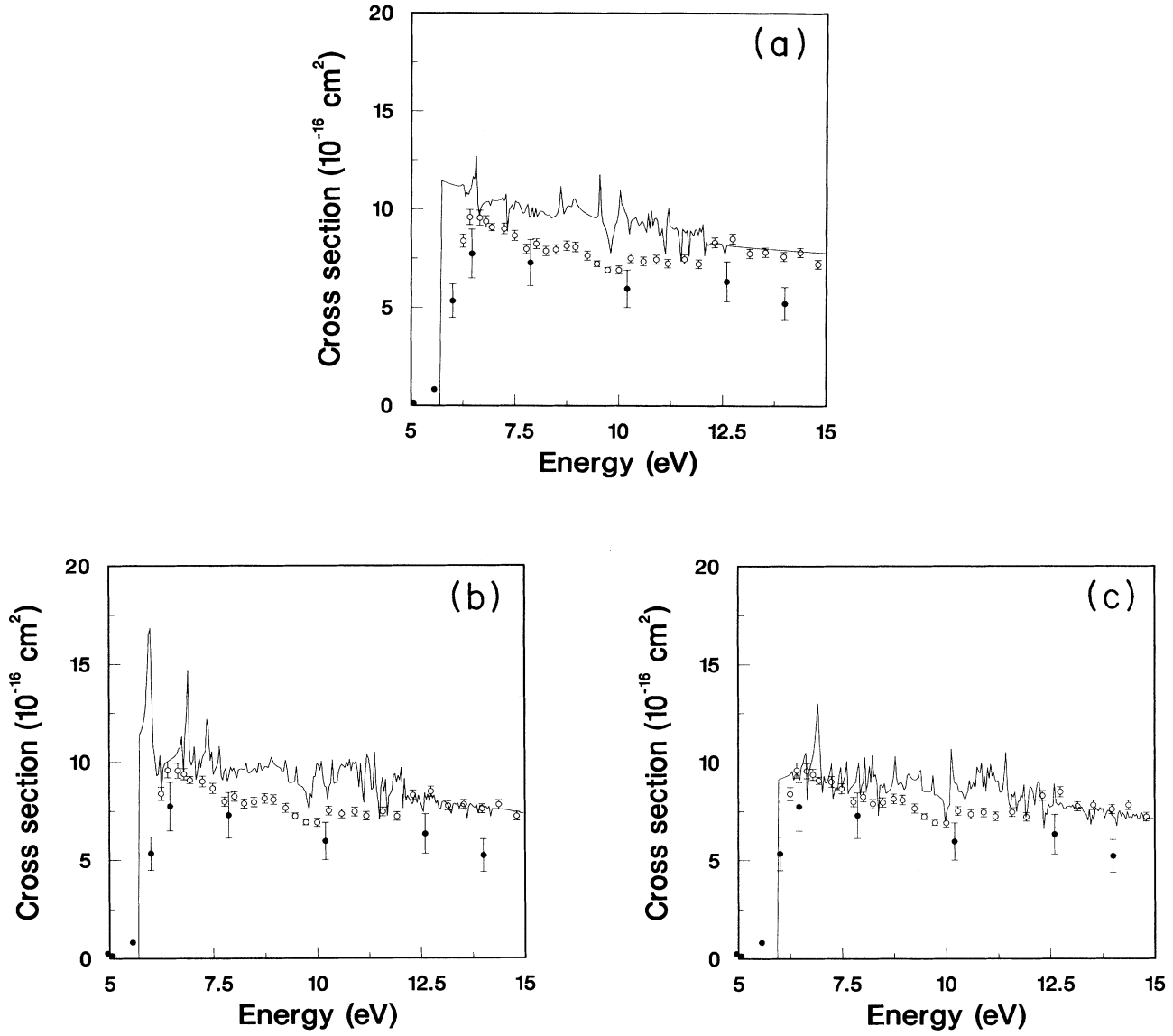

FIG. 3. Total cross section for $4s \rightarrow 4p$ transition. Solid circles, merged-beams experiment (Ref. [14]); open circles, crossed-beams experiment (Ref. [15]). (a) Solid curve, 6-state close-coupling calculation; (b) solid curve, 15-state close-coupling calculation; (c) solid curve, 31-state close-coupling calculation.

Bethe approximation in the high-energy limit, the dipole allowed cross section is directly proportional to its oscillator strength. From Table II we see that the 15-state oscillator strength is about 17% higher the multiconfiguration Hartree-Fock result for the length forms, and thus we would expect a similar overestimate in both sets of theoretical cross-section results at the higher energies. Our preliminary conclusion is that if we lower both theoretical curves by 17%, the resulting cascade-corrected results are then in very good agreement with the crossed-beams experiment, but the cascade-free results are still somewhat larger than those of the merged-beams experiment at the higher energies.

Surprisingly, however, the previous 5-state close-coupling results of Msezane and Henry [16] are in rough agreement with the merged-beams experiment for energies greater than 15 eV, and since their calculations predicted a cascade enhancement from 70% to 40% they were also in reasonable agreement with the crossed-beams experiment. Thus, for example, the 15-state cross section at 50 eV (5.0×10^{-16} cm^2) is 61% higher than the 5-state cross section (3.1×10^{16} cm^2), even though from Table II the 15-state oscillator strength is only 22% higher than the 5-state oscillator strength for the length forms. Using the original CIV3 target orbitals [16], we repeated the 5-state close-coupling calculations and found the previous results to be in error. Previously, Msezane and Henry [16] used a single-configuration description of

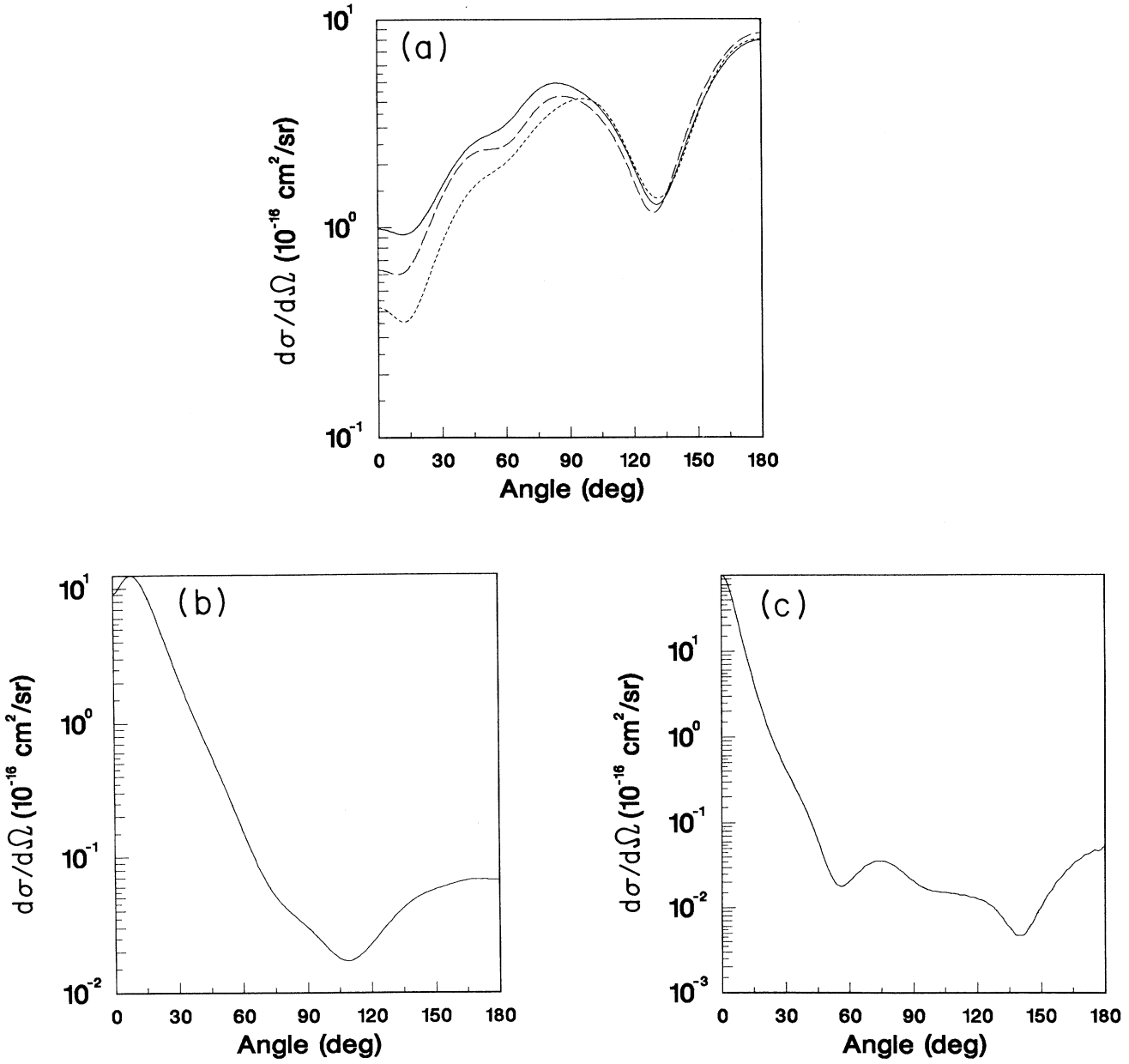

FIG. 4. Differential cross sections for $4s \rightarrow 4p$ transition. (a) 6.2-eV incident energy: solid curve, 6-state close-coupling calculation; long-dashed curve, 15-state close-coupling calculation; short-dashed curve, 31-state close-coupling calculation. (b) 20-eV incident energy: solid curve, 6-state close-coupling calculation. (c) 50-eV incident energy: solid curve, 6-state close-coupling calculation.

the $3d^{10}4s$ and $3d^{10}5s$ states, whereas it is necessary from orthogonality considerations to use a configuration-interaction description of the ^2S states. They had properly used a configuration-interaction description of the ^2D states. The new 5-state cross section results are compared with the 15-state results and the old 5-state results at four different energies in Table III. The 15-state cross section at 50 eV is now only 21% higher than the 5-state cross section (4.1×10^{-16} cm^2) and in excellent agreement with the oscillator strength difference for the length forms.

In Table IV we compare the $4s \rightarrow 4p$ cascade factors for Zn^+ calculated using the 15-state, new 5-state, and old 5-state [16] close-coupling calculations. The nondipole-allowed $4s \rightarrow 5s$ and $4s \rightarrow 4d$ excitation cross sections, which enter the cascade estimate, are strongly reduced in magnitude in going from the 5-state to the 15-state calculations. The differences found in the 5- and 15-state results are due mainly to the different target ion atomic structures. As mentioned in Sec. II, we believe

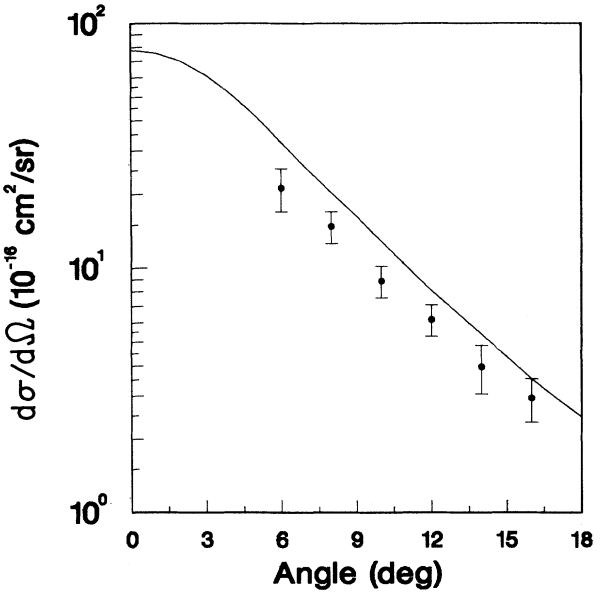

FIG. 5. Differential cross section for $4s \rightarrow 4p$ transition. Solid curve, 6-state close-coupling calculation; solid circles, energy-loss crossed-beams experiment (Ref. [28]).

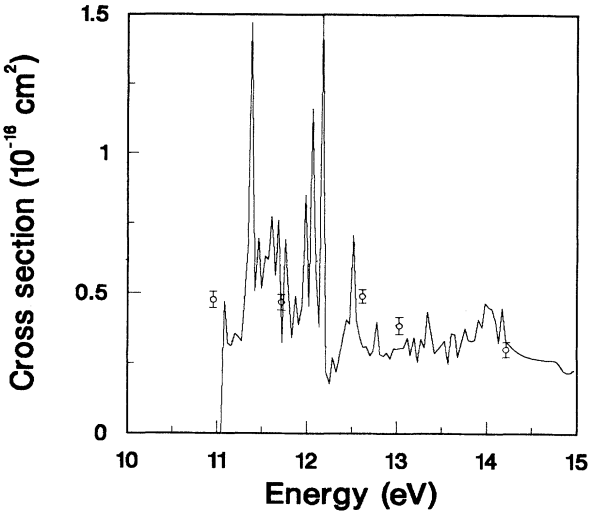

FIG. 7. Total cross section for $4s \rightarrow 5s$ transition. Solid curve, 15-state close-coupling calculation; open circles, crossed-beams experiment (Ref. [15]).

that the target wave functions associated with the 15-state calculations are the superior based on better energy level agreement with experiment. We thus conclude that our best estimate is a 15–20 % cascade enhancement for the $4s \rightarrow 4p$ excitation, as shown by the theory curves in Fig. 2. The fact that comparison of the cascade-enhanced crossed-beams experiment and the cascade-free merged-beams experiment indicates a much larger cascade factor is a puzzle.

To further check our $4s \rightarrow 4p$ cross-section results we carried out both a 6-state and a 31-state close-coupling calculation using radial orbitals from the modified version of SUPERSTRUCTURE [17], optimized for a 15-LS-term configuration-interaction (CI) calculation for Zn^+. The 6-state close-coupling calculation includes all 6 LS terms of the $3d^{10}4s$, $3d^{10}4p$, $3d^9 4s^2$, $3d^{10}5s$, $3d^{10}4d$, and $3d^{10}5p$ configurations. The 6-state calculation uses the same CI basis expansion for the target as the 15-state calculation. The 31-state close-coupling calculation augments the 15-state one with all 16 LS terms from the $3d^{10}4f$ and $3d^9 4s4d$ configurations. Since more configurations are included, the 31-state calculation has a slightly different CI basis expansion for the target than the one used for the 6- and 15-state calculations. For comparison in the threshold energy region, the 6-, 15-, and 31-state close-coupling calculations are presented in Fig. 3. The effect of including more states in the expansion appears to have little effect on the nonresonant background cross section. Given that more resonances are being added as the expansion increases, the reproducibility of the relatively weak resonance structures in the $4s \rightarrow 4p$ cross section seems to be good. There are certain anomalies, however, like the large resonance at threshold in the 15-state calculation which disappears in the 31-state calculation. We attribute this anomaly to small changes in both the N-electron target thresholds and the $(N+1)$-electron resonance positions which moves the structure from just above to just below threshold.

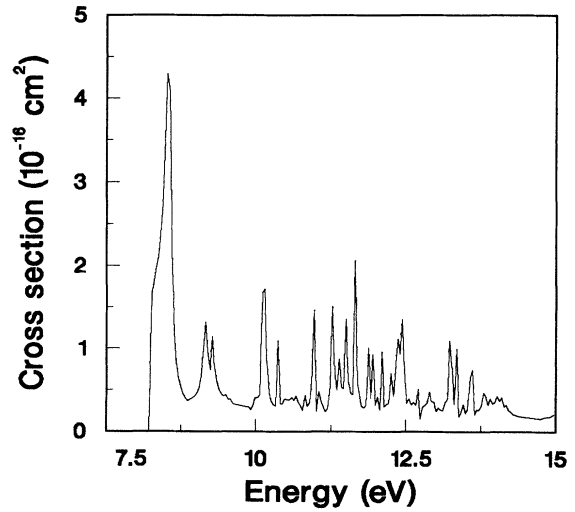

FIG. 6. Total cross section for $3d \rightarrow 4s$ transition. Solid curve, 15-state close-coupling calculation.

Since partial cross sections for the $4s \rightarrow 4p$ excitation in Zn^+ were needed to analyze the merged beams experiment [14], complete differential cross sections at 6.2-, 20-, and 50-eV incident energy have been calculated and are shown in Fig. 4. At 6.2 eV the partial cross section in the forward direction approximately equals the partial cross section in the backward direction. There is also surprisingly good agreement between the 6-, 15-, and 31-state close-coupling calculations at this low energy. At 20 and 50 eV the partial cross section in the forward direction

dominates and the agreement between the 6-, 15-, and 31-state calculations is so close only one curve is drawn in the two figures. At 20 and 50 eV the close-coupling results from partial waves $L=0-20$ are supplemented by 2-state distorted-wave calculations, using the same 15-state target expansion, for $L=21-80$ obtained using the code DSTWAV [2] developed at University College London. The close-coupling, distorted-wave, and atomic structure codes have all been modified so that either Condon-Shortley or Fano phase convention can be used throughout any specific collision cross-section calculation. We compare the close-coupling–distorted-wave differential cross sections at 50 eV with an energy-loss crossed-beams experiment [28] in Fig. 5. The relative crossed-beams measurements for Zn^+ are normalized at $\theta=12°$ to measurements for Mg^+, which in turn are matched at $\theta=12°$ to the 5-state close-coupling calculations [16] for Mg^+. With the proper inclusion of the Coulomb phase factor [29], the slope of the small-angle differential cross section has now been corrected and as shown in Fig. 4 is in relative agreement with experiment.

The 15-state close-coupling calculations for the $3d \rightarrow 4s$ and $4s \rightarrow 5s$ excitation cross sections of Zn^+ are shown in Figs. 6 and 7, where comparison with the crossed-beams experiment [15] is made for the $4s \rightarrow 5s$ transition. As expected the resonance structures seen in Figs. 6 and 7 are relatively strong for these non-dipole-allowed transitions. Due to the finite energy-grid spacing of about 0.04 eV, caution must be exercised in using the peak heights of narrow spikes on the figures.

IV. SUMMARY

Excitation cross sections for Zn^+ calculated in a multiple-LS-term close-coupling approximation have been compared with recent atomic-collision experiments. The accuracy of the target-state wave functions for Zn^+ has been investigated by comparing energy levels with experiment and oscillator strengths with other calculations and is judged to be approximately 20%. For the $4s \rightarrow 4p$ dipole-allowed excitation cross section good agreement between theory and a crossed-beams experiment is obtained over a wide energy range, once allowance for calculational uncertainties and cascade effects are made. Good agreement between theory and a merged-beams experiment is obtained in the threshold energy range, once the angle-dependent nature of the measurements is taken into account. The discrepancy at the higher energies between the cascade-free theory and the merged-beams experiment appears to be real and thus is still a puzzle. In conclusion, the further development of the atomic-collision experiments, especially in regard to mapping out resonance structures at high resolution, promises to provide a strong test of our calculational ability to model accurately atomic structures and collisional dynamics.

ACKNOWLEDGMENTS

We would like to thank the members of the Opacity Project for providing us with the latest version of the RMATRX code and to A. Chutjian for providing us with the merged-beams data prior to publication. This work was supported by the U.S. Department of Energy under Grant No. DE-FG05-86ER53217 between the Office of Fusion Energy and Auburn University, Contract No. DE-AC05-84OR21400 between the Office of Fusion Energy and Martin Marietta Energy Systems, Inc., and Grant No. DE-FG05-90ER14134 between the Division of Chemical Sciences and Auburn University.

[1] N. F. Mott and H. S. W. Massey, *The Theory of Atomic Collisions* (Oxford University Press, London, 1965).
[2] W. Eissner and M. J. Seaton, J. Phys. B **5**, 2187 (1972).
[3] M. A. Crees, M. J. Seaton, and P. M. H. Wilson, Comput. Phys. Commun. **15**, 23 (1978).
[4] P. G. Burke, A. Hibbert, and W. D. Robb, J. Phys. B **4**, 153 (1971).
[5] K. A. Berrington, P. G. Burke, M. Le Dourneuf, W. D. Robb, K. T. Taylor, and Vo Ky Lan, Comput. Phys. Commun. **14**, 367 (1978).
[6] E. R. Smith and R. J. W. Henry, Phys. Rev. A **7**, 1585 (1973).
[7] R. J. W. Henry, S. P. Rountree, and E. R. Smith, Comput. Phys. Commun. **23**, 233 (1981).
[8] N. S. Scott and P. G. Burke, J. Phys. B **13**, 4299 (1980).
[9] N. S. Scott and K. T. Taylor, Comput. Phys. Commun. **25**, 347 (1982).
[10] P. H. Norrington and I. P. Grant, J. Phys. B **20**, 4869 (1987).
[11] R. A. Phaneuf, in *Atomic Processes in Electron-Ion and Ion-Ion Collisions,* edited by F. Brouillard (Plenum, New York, 1986), p. 117.
[12] R. E. Marrs, M. A. Levine, D. A. Knapp, and J. R. Henderson, Phys. Rev. Lett. **60**, 1715 (1988).
[13] E. K. Wahlin, J. S. Thompson, G. H. Dunn, R. A. Phaneuf, D. C. Gregory, and A. C. H. Smith, Phys. Rev. Lett. **66**, 157 (1991).
[14] S. J. Smith, K. F. Man, R. J. Mawhorter, I. D. Williams, and A. Chutjian, Phys. Rev. Lett. **67**, 30 (1991).
[15] W. T. Rogers, G. H. Dunn, J. Ostgaard Olsen, M. Reading, and G. Stefani, Phys. Rev. **A25**, 681 (1982).
[16] A. Z. Msezane and R. J. W. Henry, Phys. Rev. A **25**, 692 (1982).
[17] W. Eissner, M. Jones, and H. Nussbaumer, Comput. Phys. Commun. **8**, 270 (1974).
[18] A. Burgess, H. E. Mason, and J. A. Tully, Astron. Astrophys. **217**, 319 (1989).
[19] A. Hibbert, Comput. Phys. Commun. **9**, 141 (1975).
[20] C. E. Moore, *Atomic Energy Levels,* Natl. Bur. Stand. Ref. Data Ser., Natl. Bur. Stand. (U.S.) Circ. No. 35 (U.S. GPO, Washington, DC, 1971), Vol. II.
[21] C. Froese-Fischer, J. Phys. B **10**, 1241 (1977).
[22] K. A. Berrington, P. G. Burke, K. Butler, M. J. Seaton, P. J. Storey, K. T. Taylor, and Yu Yan, J. Phys. B **20**, 6379

(1987).
[23] M. J. Seaton (unpublished)
[24] A. Burgess, J. Phys. B **7**, L364 (1974).
[25] V. M. Burke and M. J. Seaton, J. Phys. B **19**, L527 (1986).
[26] D. C. Griffin and M. S. Pindzola, Phys. Rev. A **42**, 248 (1990).
[27] A. Burgess and J. A. Tully, J. Phys. B **11**, 4271 (1978).
[28] I. D. Williams, A. Chutjian, and R. J. Mawhorter, J. Phys. B **19**, 2189 (1986).
[29] J. Mitroy, Phys. Rev. A **37**, 649 (1988).